Cocontraction in reaching simulations with third order muscle activation dynamics

Tiina Murtola, Christopher Richards
Royal Veterinary College, London, United Kingdom
tmurtola@rvc.ac.uk, ctrichards@rvc.ac.uk

1 Introduction

Controlling upper limb reaching movements is challenging, partly due to nonlinearities, uncertainties, and delays. Joint stiffness control has been proposed to address some of the issues (e.g., [1,2]), grossly explaining agonist-antagonist cocontraction observed in humans. To study the effect of intrinsic muscle properties on impedance control, we compare reaching performance of a simple arm model comprising a standard activation model versus a high-order activation model that mimics muscle dynamics more closely [3]. We expect higher-order activation dynamics to affect the motor controller's optimal tuning and to increase cocontraction, helping to further explain natural cocontraction in reaching.

2 The arm model

An anatomically simplified planar model is used for tractability and to simplify control. The model consists of four rigid links: a stationary ground link and three arm links that move in the horizontal plane. The model configuration at time t is described by the joint angles $\mathbf{q}(t) = (q_1, q_2, q_3)$, where q_1 corresponds to the shoulder, q_2 to the elbow, and q_3 to the wrist. The position of end of the hand link, $\mathbf{x}(t) = (x_1, x_2)$, is tracked for the reaching movements. The model arm is controlled by feeding excitation signals to three agonist-antagonist muscle pairs. Each muscle crosses a single joint, functioning as its flexor or extensor[1].

Muscle contraction generates joint torques

$$\mathbf{T} = \mathbf{R}(\mathbf{q})\,\mathbf{F}(\mathbf{l},\dot{\mathbf{l}})\,\mathbf{a}(\mathbf{u}), \tag{1}$$

where $\mathbf{a}(\mathbf{u})$ is a vector of muscle activation states in response to the excitation vector $\mathbf{u}(t)$, $\mathbf{F}(\mathbf{l},\dot{\mathbf{l}})$ is a diagonal matrix mapping the activations to muscle forces using a Hill-type model to account for nonlinear force modulation at muscle length $\mathbf{l}(\mathbf{q})$ and contraction velocity $\dot{\mathbf{l}}(\mathbf{q},\dot{\mathbf{q}})$, and $\mathbf{R}(\mathbf{q})$ is a matrix of moment arms which maps the muscle forces to torques.

Two activation dynamics models (ADMs) are used: (1) an experimentally validated third order model [3],

$$\begin{aligned}
\dot{\mathbf{a}}_1 + \tfrac{1}{\alpha_1}\left(\beta_1 + [1-\beta_1]\mathbf{u}\right)\mathbf{a}_1 &= \tfrac{1}{\alpha_1}\mathbf{u},\\
\dot{\mathbf{a}}_2 + \tfrac{1}{\alpha_2}\left(\beta_2 + [1-\beta_2]\mathbf{a}_1\right)\mathbf{a}_2 &= \tfrac{1}{\alpha_2}\mathbf{a}_1,\\
\dot{\mathbf{a}} + \tfrac{1}{\alpha_3}\left(\beta_3 + [1-\beta_3]\mathbf{a}_2\right)\mathbf{a} &= \tfrac{1}{\alpha_3}\mathbf{a}_2,
\end{aligned} \tag{2}$$

[1] Or, technically, as a horizontal adductor/abductor at the shoulder

where $\mathbf{a}_1$ and $\mathbf{a}_2$ are intermediate state variables and α_i and β_i, $i = 1,2,3$, are time constants and nonlinearity parameters, respectively, and (2) a simpler first order model with time constant α,

$$\dot{\mathbf{a}} + \tfrac{1}{\alpha}\mathbf{a} = \tfrac{1}{\alpha}\mathbf{u}. \tag{3}$$

The constants α_i, β_i, and α were set so that the half-relaxation time of the twitch responses is 82 ms.

3 Reaching tasks and control

Four targets at an equal distance but different directions from a fixed initial position are used for the reaching task. The desired trajectory, $\mathbf{x}_d(t)$, of each reach is a straight line with the bell-shaped tangential velocity profile defined by the minimum jerk theory [4]. The movement of the model along this trajectory is controlled with a PD controller (Figure 1) which computes the desired joint torques, $\mathbf{T}_d$, from the error between desired and predicted states at time $t+\tau$,

$$\mathbf{T}_d = \mathbf{K}_p\hat{\mathbf{J}}^{\dagger}(\mathbf{x}_d - \hat{\mathbf{x}}) + \mathbf{K}_v\hat{\mathbf{J}}^{\dagger}(\dot{\mathbf{x}}_d - \dot{\hat{\mathbf{x}}}), \tag{4}$$

where $\mathbf{K}_p = \mathrm{diag}(k_{p1}, k_{p1}, k_{p1})$ and $\mathbf{K}_v = \mathrm{diag}(k_{v1}, k_{v1}, k_{v1})$ are gains, $\hat{\mathbf{J}}^{\dagger} = \mathbf{J}^{\dagger}(\hat{\mathbf{q}})$ is the pseudo-inverse of the Jacobian at the predicted state, and $\hat{\mathbf{x}}$ denotes the predicted position. Prediction is used to mitigate the destabilising effects of the delays inherent in the ADMs. A copy of the arm model is

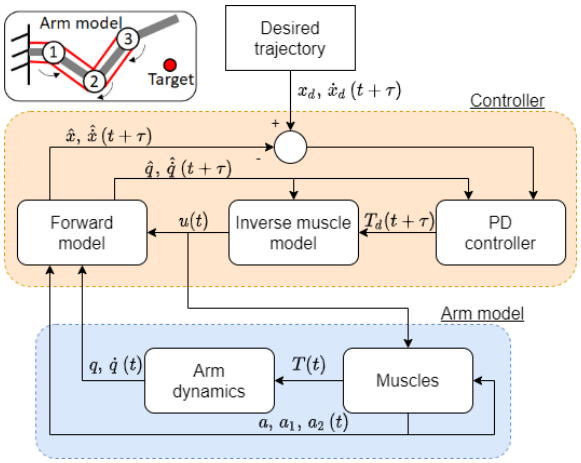

Figure 1: The arm model (inset) is controlled using the prediction of a forward model, a PD controller to determine desired joint torques, and an inverse muscle model to convert torques to muscle excitations.

used as a forward model but with the excitation signals $\mathbf{u}$ kept constant between t and $t+\tau$.

Eq. (1) does not have a unique inverse both due to the possibility of cocontraction and because an activation state can result from multiple past excitation patterns. Therefore, the inverse muscle model used in the control loop (Figure 1) approximates the ADMs with a constant delay so that $\mathbf{a}(t+\tau) = \mathbf{u}(t)$, and it also assumes that no coexcitation is allowed, that is, if a muscle is excited ($u_i > 0$) then its antagonist will have $u_j = 0$.

4 Results

The gains $\mathbf{K}_p$ and $\mathbf{K}_v$ as well as the delay constant τ were optimised numerically by minimising the average error between the actual and planned trajectories. When the first order ADM was used, the optimal $\tau = 6$ ms (time steps of 2 ms were used for all simulations), whereas for the model with the third order ADM, a notably longer window of prediction was required with $\tau = 34$ ms.

The two model versions follow nearly identical trajectories and finish in the same configuration, but the model with the third order ADM performs optimally when roughly equal weights are placed on the positional errors of the elbow and wrist, whereas with the first order ADM, the elbow is emphasised over the wrist (Figure 2). There is also a decrease in the optimal velocity gains when the third order ADM is used.

While the external performance of the model does not depend on the choice of ADM, differences in the control parameters are reflected in the internal state of the system. There are, in particular, notable changes in the patterns of cocontraction (i.e., simultaneous force production) of the agonist-antagonist muscle pairs (Figure 3). The level of cocontraction increases when the third order ADM is used, but the effect is not uniform across all joints. Cocontraction of the muscles crossing the shoulder joint increases from negligible (max. 3%) to noticeable (max. 25%) levels while the relative changes in the cocontraction of the muscles crossing the wrist are more moderate. The combination of lower velocity gains and higher cocontraction with the third order ADM suggests a shift in control strategy: movement is stabilised by stiffening joints instead of utilising $\mathbf{K}_v$ to effect damping, possibly because the combination of increasing nonlinearity the model and a larger τ makes velocity prediction less reliable.

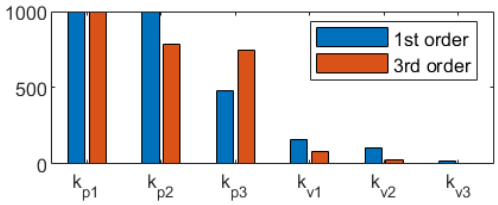

Figure 2: Optimal feedback gains for the PD controller for muscles with first and third order activation dynamics.

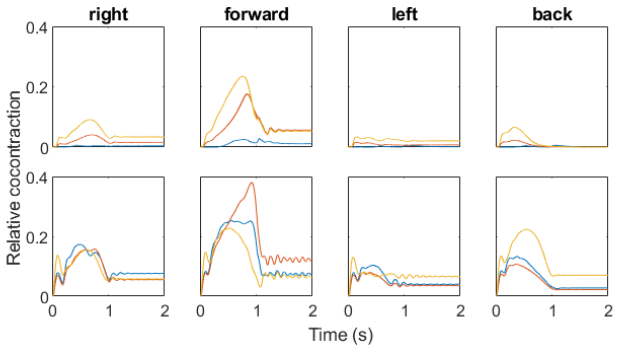

Figure 3: Cocontraction of muscle pairs crossing the shoulder (blue), elbow (red) and wrist (yellow) as a fraction of isometric strength in reaches in four directions. Top row: first order ADM. Bottom: third order ADM.

Some characteristics of cocontraction are independent of ADM. In the case where the target lies directly in front, a high level of cocontraction is retained, likely because a nearly straight arm is required to reach the target. This makes $\mathbf{x}$ harder to control regardless of ADM as only the shoulder joint can be used effectively and the length of the arm amplifies any errors made by the controller.

5 Conclusions

We tested how muscle activation properties influence neuromuscular control of reaching. As expected, the inherent delays of our physiologically-realistic high-order model changed the optimal control strategy, requiring altered feedback gains and longer prediction times. Additionally, cocontraction emerged as a strategy to deal with an imperfect controller, especially inaccuracies in the inverse muscle model. Our simulations therefore suggest that muscle activation properties influence motor control and that reaching is robust to physiological delays, but at the cost of increased cocontraction.

6 Acknowledgements

This work was funded by a Wellcome Trust Investigator Award 215618/Z/19/Z.

References

[1] N. Hogan. Adaptive control of mechanical impedance by coactivation of antagonist muscles. *IEEE Transactions on Automatic Control*, 29(8):681–690, 1984.

[2] D. Mitrovic, S. Klanke, R. Osu, M. Kawato, and S. Vijayakumar. A computational model of limb impedance control based on principles of internal model uncertainty. *PloS ONE*, 5(10):e13601, 2010.

[3] S.S.M. Lee, M. de Boef Miara, A.S. Arnold, A.A. Biewener, and J.M. Wakeling. EMG analysis tuned for determining the timing and level of activation in different motor units. *Journal of Electromyography and Kinesiology*, 21(4):557–565, 2011.

[4] T. Flash and N. Hogan. The coordination of arm movements: an experimentally confirmed mathematical model. *Journal of Neuroscience*, 5(7):1688–1703, 1985.